arXiv:hep-lat/9608053v1 11 Aug 1996

HU Berlin–EP–96/36

Dynamical Wilson fermions and the problem of the chiral limit in compact lattice QED†

A. Hoferichter[1], V.K. Mitrjushkin[1] ‡, M. Müller-Preussker[1] and H. Stüben[2]

[1] *Institut für Physik, Humboldt-Universität zu Berlin, Germany*
[2] *Konrad-Zuse-Zentrum für Informationstechnik Berlin, Germany*

Abstract

We compare the approach to the chiral transition line $\kappa_c(\beta)$ in quenched and full compact lattice QED with Wilson fermions within the confinement phase, especially in the pseudoscalar sector of the theory. We show that in the strong coupling limit ($\beta = 0$) the quenched theory is a good approximation to the full one, in contrast to the case of $\beta = 0.8$. At the larger β-value the transition in the full theory is inconsistent with the zero–mass limit of the pseudoscalar particle, thus prohibiting the definition of a chiral limit.

1 Introduction and model description

Chiral symmetry as a major concept in continuum quantum field theory has remained a problematic topic in lattice gauge theories over the years. It is well-known, that for Wilson fermions chiral symmetry is explicitly broken in QCD and QED on the lattice [1, 2]. Hopefully, it can be recovered by fine-tuning of parameters in the continuum limit. Then some line $\kappa_c(\beta)$ in the phase diagram is associated with the chiral limit of the theory. On the other hand, for non-vanishing lattice spacing only a partial restoration of chiral symmetry at $\kappa = \kappa_c(\beta)$ is possible with Wilson fermions [3, 4]. It is still an open question, how this mechanism of partial symmetry restoration should eventually be integrated into the general conception of spontaneously broken chiral symmetry. One cannot exclude that the breakdown of some other symmetry group governs the dynamics of the transitions at $\kappa_c(\beta)$ (e.g., [5]). Viewed in this light the vanishing of the pseudoscalar 'pion' mass m_π

†Work supported by the Deutsche Forschungsgemeinschaft under research grant Mu 932/1-4
‡Permanent address: Joint Institute for Nuclear Research, Dubna, Russia

for $\kappa \to \kappa_c(\beta)$ is a necessary but not sufficient condition for probing the chiral limit. Another point which sharpened the look on the chiral limit in QCD [6, 7] is the discussion of 'enhanced logs' due to quenching, demonstrating the rôle of dynamical fermions in chiral properties of the theory.

In this letter we are concerned with the behavior of fermionic observables close to $\kappa_c(\beta)$ in the confinement phase of compact QED. We confront the full theory with its valence approximation. Though the non-perturbative regime of compact QED is itself an interesting subject the close analogy with non-Abelian gauge theories makes it also a valuable test ground for QCD with Wilson fermions.

In the rest of the section we will introduce the model and give the main notations. Starting point is the partition function of $4d$ compact QED which reads as follows

$$Z_{QED} = \int [dU][d\bar{\psi}d\psi]\ \mathrm{e}^{-S_W(U,\ \bar{\psi},\psi)}\ , \tag{1}$$

where $S_W(U,\bar{\psi},\psi)$ denotes the standard Wilson lattice action

$$S_W = S_G(U) + S_F(U,\bar{\psi},\psi) \tag{2}$$

consisting of the plaquette action

$$S_G(U) = \beta \cdot \sum_{x;\mu>\nu} (1 - \cos\theta_{x;\mu\nu})\ , \tag{3}$$

and the fermionic part $S_F(U,\bar{\psi},\psi)$

$$\begin{aligned} S_F &= \sum_{f=1}^{2} \sum_{x,y} \bar{\psi}^f_x \mathcal{M}_{xy} \psi^f_y \\ \mathcal{M}_{xy} &\equiv \hat{1} - \kappa \cdot \left[\delta_{y,x+\hat{\mu}} \cdot (\hat{1}-\gamma_\mu) \cdot U_{x\mu} + \delta_{y,x-\hat{\mu}} \cdot (\hat{1}+\gamma_\mu) \cdot U^\dagger_{x-\hat{\mu},\mu}\right]\ , \end{aligned} \tag{4}$$

with $\beta = 1/g^2_{bare}$, and $U_{x\mu} = \exp(i\theta_{x\mu})$, $\theta_{x\mu} \in (-\pi,\pi]$ represent the link fields. The plaquette angles $\theta_{x;\,\mu\nu}$ in eq.(3) are given by $\theta_{x;\,\mu\nu} = \theta_{x;\,\mu} + \theta_{x+\hat{\mu};\,\nu} - \theta_{x+\hat{\nu};\,\mu} - \theta_{x;\,\nu}$. In the fermionic part of the action $\mathcal{M}_{xy}$ denotes Wilson's fermionic matrix with the hopping parameter κ and the flavor–index f.

The phase diagram of this model has been studied in [8]. Within the region of values $0 \le \kappa \le 0.30$ the existence of four phases has been established. The line $\kappa_c(\beta)$ separates both the confinement phase ($0 \le \beta < \beta_0$ with $\beta_0 \simeq 1.01$) and the Coulomb phase ($\beta > \beta_0$) from two upper phases (which we called the 3^{rd} phase at weak and the 4^{th} phase at strong coupling). At $\beta = 0.8$ it was observed that the scalar condensate $\langle\bar{\psi}\psi\rangle$ has a discontinuity at κ_c, therefore we called the transition at this point a 1^{st} order transition. However, the κ–dependence of the pseudoscalar observables was not studied in detail.

The fermionic observables to be discussed are the pion norm

$$\langle \Pi \rangle = \frac{1}{4V} \cdot \Big\langle \mathrm{Tr}\Big(\mathcal{M}^{-1} \gamma_5 \mathcal{M}^{-1} \gamma_5 \Big) \Big\rangle_G \ , \tag{5}$$

being a good indicator for small eigenvalues of the fermionic matrix and the mass of the pseudoscalar particle m_π, which is extracted from the pseudoscalar zero-momentum correlator

$$\begin{aligned} \Gamma(\tau) &= -\frac{1}{N_s^6} \cdot \sum_{\vec{x},\vec{y}} \Big\langle \overline{\psi}\gamma_5\psi(\tau,\vec{x}) \cdot \overline{\psi}\gamma_5\psi(0,\vec{y}) \Big\rangle \\ &\equiv \frac{1}{N_s^6} \cdot \sum_{\vec{x},\vec{y}} \Big\langle \Big\{ \mathrm{Sp}\Big(\mathcal{M}^{-1}_{xy}\gamma_5 \mathcal{M}^{-1}_{yx}\gamma_5 \Big) - \mathrm{Sp}\Big(\mathcal{M}^{-1}_{xx}\gamma_5 \Big) \cdot \mathrm{Sp}\Big(\mathcal{M}^{-1}_{yy}\gamma_5 \Big) \Big\} \Big\rangle_G \end{aligned} \tag{6}$$

In eqs.(5,6) $\langle\ \rangle_G$ indicates averaging over gauge field configurations, and $V = N_\tau \cdot N_s^3$ is the number of sites. Sp means the trace with respect to the Dirac indices. Other observables like $\langle \rho_{mon} \rangle$ – the density of DeGrand-Toussaint monopoles [9] – and the photon correlator have also been determined.

Formally we define the bare fermion mass parameter m_q by

$$m_q = \frac{1}{2}\Big(\frac{1}{\kappa} - \frac{1}{\kappa_c(\beta)} \Big) \ . \tag{7}$$

For the determination of the κ_c see below.

In this work we discuss data from an $8^3 \times 16$ lattice at two values of β within the confinement phase. For the production of dynamical gauge field configurations we employed a CRAY-T3D implementation of the Hybrid Monte Carlo (HMC) method. A detailed presentation of algorithmic issues, like the tuning of the HMC parameters when approaching κ_c is deferred to [10].

2 Effects of dynamical Wilson fermions

First, we shall discuss the behavior of the bulk observable $\langle \Pi \rangle$ when approaching the line $\kappa_c(\beta)$ at fixed β within the range $0 \le \beta < \beta_0$ (confinement phase). As in our previous work for representative β–values we have chosen $\beta = 0.8$ and the strong coupling limit $\beta = 0$. In the latter limit the comparison with analytical results is possible (e.g., [3, 11]).

Provided the pseudoscalar mass vanishes for $m_q \to 0$ it will yield the dominant contribution to the pion norm $\langle \Pi \rangle \sim 1/m_\pi^2$. In case of a PCAC-like relation between m_π and m_q the pion norm can be expressed in the following form

$$\langle \Pi \rangle = \frac{C_0}{m_q} + C_1 \ , \quad m_q \to 0 \ , \tag{8}$$

where $C_0 > 0$ – up to a factor – is the subtracted chiral condensate [12] (see also [13]). $C_1 = \langle \Pi_m \rangle$ is the contribution of the massive modes.

In Figure 1 data for the quenched and dynamical cases at $\beta = 0$ are presented to view. The quenched approximation follows the m_q–dependence of the full pion norm $\langle \Pi \rangle$ very well, even quantitatively. As $m_q \to 0+$ the singularity of $\langle \Pi \rangle$ at $\beta = 0$ is well described in both cases by eq.(8) with values of C_0, C_1 listed in Table 1. Note that C_0 and C_1 differ somewhat for the quenched and dynamical cases and could not be forced to coincide by shifting κ_c. The quenched and dynamical theories nevertheless exhibit the same functional dependence on m_q when $m_q \to 0$.

For $\kappa \gtrsim \kappa_c$ the averages of fermionic bulk observables in the quenched approximation become poorly defined due to large fluctuations caused by 'exceptional' configurations [13, 14]. In the theory with dynamical fermions we also observe increasing fluctuations of, e.g., Π when κ is tuned towards κ_c from below. We were able to proceed to $\kappa = 0.242$ ($m_q \sim 0.0253$) at $\beta = 0$, before being faced with serious problems with the acceptance rate of the HMC method.

The situation changes drastically when the gauge coupling β is increased. By examining time histories of Π and other observables at $\beta = 0.8$ we observe the formation of metastable states in a 'critical' region around κ_c in the presence of dynamical fermions. Figure 2a illustrates a clearly double peaked distribution of Π close to κ_c for the case of dynamical fermions.

As an example concerning the behavior of other observables, the dependence of $\langle \rho_{mon} \rangle$ on κ is depicted in Figure 2b. The evolution of $\langle \rho_{mon} \rangle$ resembles the situation of the confinement–deconfinement transition at β_0 for a sufficiently small fixed κ and varying β [8].

Measurements of the effective photon energy extracted from plaquette–plaquette correlators for non-zero momentum confirm that in the case of dynamical fermions the system undergoes a confinement–deconfinement transition at κ_c (see [8]). With increasing κ the effective energy of the photon rapidly decreases around κ_c and becomes well consistent with the lattice dispersion relation for a zero–mass photon.

We used further 'order parameters' to determine κ_c and to make sure that there are no other transition points different from that within the investigated κ–range. For example, the variance $\sigma^2(\Pi)$ which is a suitable parameter to locate the line $\kappa_c(\beta)$ within the Coulomb phase [8] peaks at the same κ_c.

In Figure 3 as counterpart of Figure 1 we confront the dependence of $\langle \Pi \rangle$ on m_q in the quenched approximation with the corresponding data when dynamical fermions are taken into account. The general features of the valence approximation at $\beta = 0.8$ are the same as at $\beta = 0$. $\langle \Pi \rangle$ has a singularity for $m_q \to 0+$ described very well by eq.(8) (dashed line in Figure 3) with parameters C_0; C_1 given in Table 1. However, the effect of the fermionic determinant is now seen as a qualitative change in the behavior of the pion norm, which does not behave as $\sim 1/m_q$ but rather exhibits a finite discontinuity accompanied by a metastable behavior (cf. Figure 2a) around κ_c. In the quenched theory averages of Π become

statistically not well–defined for $\kappa \gtrsim \kappa_c$, as in the case of $\beta = 0$, while in the dynamical case at $\beta = 0.8$ there is no problem to go beyond κ_c (i.e., into the 3^{rd} phase [8]). The dependence of $\langle \Pi \rangle$ on κ (respectively m_q) is not symmetric around κ_c.

To substantiate the emerging picture at $\beta = 0$ and $\beta = 0.8$ we will discuss the evolution of the pseudoscalar mass m_π when $\kappa \to \kappa_c$. We present in Figure 4 the dependence of m_π^2 on κ for the full and quenched theories on an $8^3 \times 16$ lattice at $\beta = 0$. The quenched data for κ very close to κ_c are obtained by an improved estimator of m_π [13] in order to increase the signal-to-noise ratio. Since the existence of a massless pseudoscalar particle is predicted by strong coupling arguments [3] we extrapolate our dynamical data for m_π^2 linearly to zero in order to determine $\kappa_c(\beta = 0)$ as we have done in the quenched case [13]. In Table 1 we list the values of κ_c obtained for the dynamical and the quenched cases on an $8^3 \times 16$ lattice. The extrapolated values of κ_c for the quenched case are well consistent with the prediction at strong coupling [3]. In both, quenched and dynamical cases we observe the following dependence of m_π^2 on the hopping parameter when approaching κ_c from below

$$m_\pi^2 \sim \left(1 - \frac{\kappa}{\kappa_c}\right) , \quad \kappa \leq \kappa_c \ , \tag{9}$$

which in this limit transforms into a PCAC–like relation between m_π^2 and the bare fermion mass m_q :

$$m_\pi^2 = B \cdot m_q \ , \quad m_q \to 0 + \ . \tag{10}$$

The corresponding slopes B for the quenched and full theories coincide within the errorbars (see Table 1). Thus, Figure 4 suggests a zero-mass pseudoscalar particle to exist. However, this is a necessary but not a sufficient prerequisite for the definition of the chiral limit.

$\beta = 0$				
	κ_c	B	C_0	C_1
dynamical	0.2450(6)	4.87(5)	0.895(1)	0.88(1)
quenched	0.2502(1)	4.91(4)	0.996(2)	0.80(1)
$\beta = 0.8$				
dynamical	0.1832(3)			
quenched	0.2171(1)	3.42(3)	0.94(2)	0.72(1)

Table 1: Compilation of different parameters (see text) for the dynamical and quenched theories at $\beta = 0$ and $\beta = 0.8$ on an $8^3 \times 16$ lattice.

The corresponding behavior of m_π^2 at $\beta = 0.8$ for quenched and dynamical

fermions is plotted in Figure 5. From the inset of Figure 5 it can be seen, that as long as the quenched theory is considered the situation is fully compatible with eq.(9). Thus eq.(10) holds as in the case of $\beta = 0$. Concerning dynamical fermions, again the situation at $\beta = 0.8$ appears to be in sharp contrast to the $\beta = 0$ and to the quenched cases, as could be expected from the properties of the pion norm. By approaching the 'critical' value $\kappa_c(\beta)$ from below with dynamical fermions, the κ–dependence of m_π^2 is not linear anymore, i.e. is not compatible with eq.(9). Moreover, close to $\kappa_c(\beta)$ m_π has a comparatively large finite minimal value which would imply that a zero-mass pseudoscalar particle is not contained in the spectrum of the theory at this particular coupling. Increasing κ beyond κ_c the pseudoscalar mass starts to rise again. Note that in the vicinity of κ_c the dependence of the pseudoscalar mass on κ is different for $\kappa > \kappa_c$ and $\kappa < \kappa_c$, in accordance with the discussion of the pion norm before.

3 Conclusions and discussion

We have studied the approach to $\kappa_c(\beta)$ for two β–values within the confinement phase of the compact lattice QED with Wilson fermions comparing the full theory with its quenched approximation. We have shown the importance of vacuum polarization effects due to dynamical fermions in the context of the chiral limit.

In the strong coupling limit $\beta = 0$ the main effect of dynamical fermions seems to be a renormalization of the 'critical' value κ_c, $\kappa_c^{dyn} \neq \kappa_c^{quen}$. The functional dependence of the studied observables on κ (respectively m_q) in the limit $\kappa \to \kappa_c$ compared to the quenched approximation does not change. Our data suggest, that at $\beta = 0$ the pseudoscalar particle becomes massless when $\kappa \to \kappa_c$.

At $\beta = 0.8$ the presence of the dynamical ('sea') fermions drastically change the transition. There we have found a transition which cannot be associated with the zero-mass limit of a pseudoscalar particle anymore, in sharp contrast to the quenched case.

Naively, one would expect that the chiral limit could be established everywhere in the confinement phase when approaching the 'critical' line $\kappa_c(\beta)$. This is not the case. Therefore the question arises whether even at $\beta = 0$ the vanishing pseudoscalar mass can be interpreted as a chiral limit. An alternative scenario for the vanishing pseudoscalar mass could be the breakdown of some other symmetry than the chiral one.

Another possible conclusion from these observations is that the calculations – analytical and numerical – in the strong coupling limit $\beta = 0$ can hardly serve for the interpretation of the mechanism of the chiral transition at larger β's (at least, in this model).

These statements need further confirmation, especially on larger lattices. Here

work is in progress [10]. It is interesting to what extent the given conclusions can be generalized to the case of QCD.

Acknowledgement

V.K.M. acknowledges support by EEC–contract CHRX-CT92-0051 during his stay at Swansea University where part of this work was done. The calculations have been performed on CRAY-T3D, CRAY-YMP, CRAY-J90 at Konrad–Zuse–Zentrum Berlin and on Convex–C3820 at the computer center of Humboldt University Berlin.

References

[1] K. Wilson, Phys. Rev. **D10** (1974) 2445; in New phenomena in subnuclear physics, ed. A. Zichichi (Plenum, New York, 1977).

[2] M. Lüscher, Commun. Math. Phys. **54** (1977) 283.

[3] N. Kawamoto, Nucl. Phys. **B190** (1981) 617.

[4] N. Kawamoto and J. Smit, Nucl. Phys. **B192** (1981) 100.

[5] S. Aoki, Phys. Rev. **D30** (1984) 2653; Phys. Rev. Lett. **57** (1986) 3136; Phys. Lett. **B190** (1987) 140; UTHEP-318 (hep-lat/9509008).

[6] S. Sharpe, Nucl. Phys. **B** (Proc. Suppl.) **17** (1990) 1990; Phys. Rev. **D41** (1990) 3146.
C. Bernard and M. Golterman, Phys. Rev. **D46** (1992) 853.

[7] R. Gupta, Nucl. Phys. **B** (Proc. Suppl.) **42** (1995) 85.

[8] A. Hoferichter, V.K. Mitrjushkin, M. Müller-Preussker, Th. Neuhaus and H. Stüben, Nucl. Phys. **B434** (1995) 358.

[9] T.A. DeGrand and D. Toussaint, Phys. Rev. **D22** (1980) 2478.

[10] A. Hoferichter, V.K. Mitrjushkin, M. Müller-Preussker and H. Stüben, in preparation.

[11] J.-M. Blairon, R. Brout, F. Englert and J. Greensite,
Nucl. Phys. **B180** (1981) 439.
H. Kluberg-Stern, A. Morel and B. Petersson, Nucl. Phys. **B215** (1983) 527.

[12] M. Bochicchio, L. Maiani, G. Martinelli, G. Rossi and M. Testa,
Nucl. Phys. **B262** (1985) 331.

[13] A.Hoferichter, V.K.Mitrjushkin and M.Müller-Preussker, Nucl. Phys. **B** (Proc. Suppl.) **42** (1995) 669.
A.Hoferichter, V.K.Mitrjushkin and M.Müller-Preussker, hep-lat/9506006 to appear in Z. f. Physik C.

[14] Ph. De Forcrand, A. König, K.-H. Mütter, K. Schilling and R. Sommer, in: Proc. Intern. Symp. on Lattice gauge theory (Brookhaven, 1986), (Plenum, New York, 1987).
Ph. De Forcrand, R. Gupta, S. Güsken, K.-H. Mütter, A. Patel, K. Schilling and R. Sommer, Phys. Lett. **200B** (1988) 143.

Figure captions

Figure 1: The pion norm $\langle\Pi\rangle$ vs. m_q at $\beta = 0$. The curved lines correspond to eq.(8) with C_0, C_1 given in Table 1.

Figure 2: The unnormalized distribution of Π at $\beta = 0.8$ in the vicinity of κ_c (**a**) and $\langle\rho_{mon}\rangle$ in dependence of κ at the same value of β (**b**) both for the theory with dynamical fermions.

Figure 3: Counterpart to Figure 1 at $\beta = 0.8$.

Figure 4: The κ–dependence of m_π^2 for the quenched and dynamical theories at $\beta = 0$ on an $8^3 \times 16$ lattice. The broken lines represent linear fits.

Figure 5: The behavior of m_π^2 around κ_c at $\beta = 0.8$. The κ-scale of the smaller plot is condensed in order to permit a direct comparison between the dynamical and quenched data. The straight line corresponds to a linear fit of the quenched data.

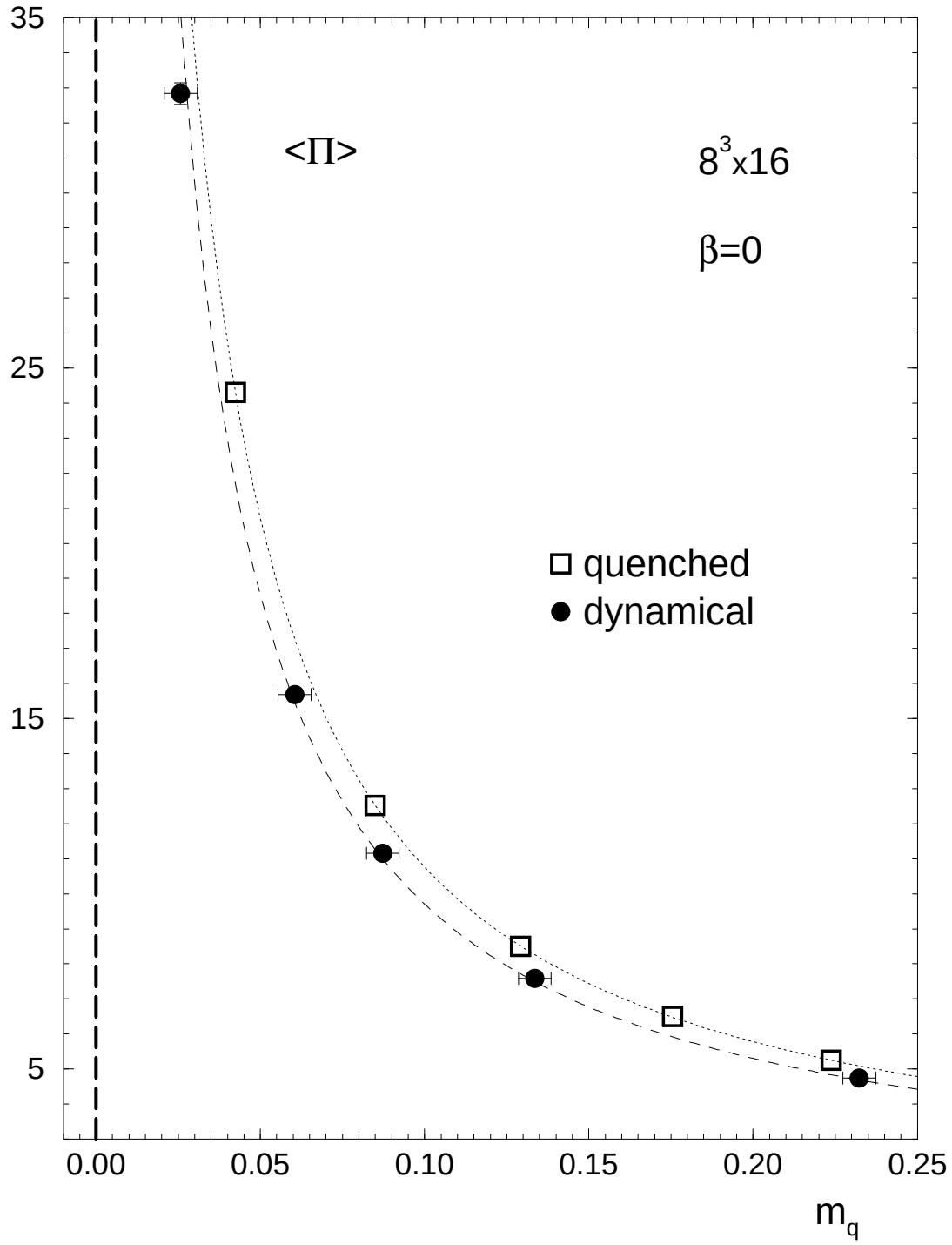

Figure 1: The pion norm $\langle \Pi \rangle$ vs. m_q at $\beta = 0$. The curved lines correspond to eq.(8) with C_0, C_1 given in Table 1.

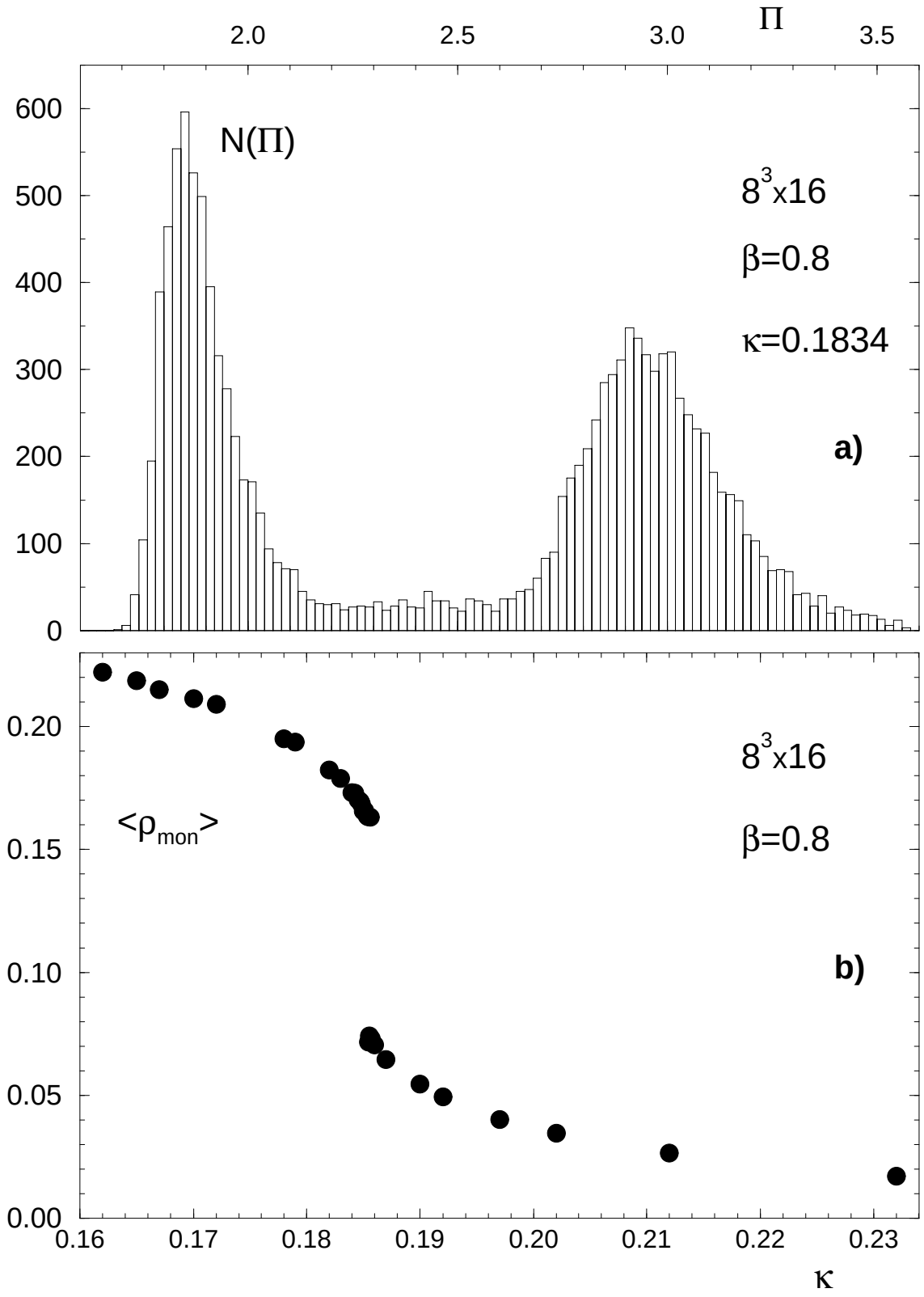

Figure 2: The unnormalized distribution of Π at $\beta = 0.8$ in the vicinity of κ_c (**a**) and $\langle \rho_{mon} \rangle$ in dependence of κ at the same value of β (**b**) both for the theory with dynamical fermions.

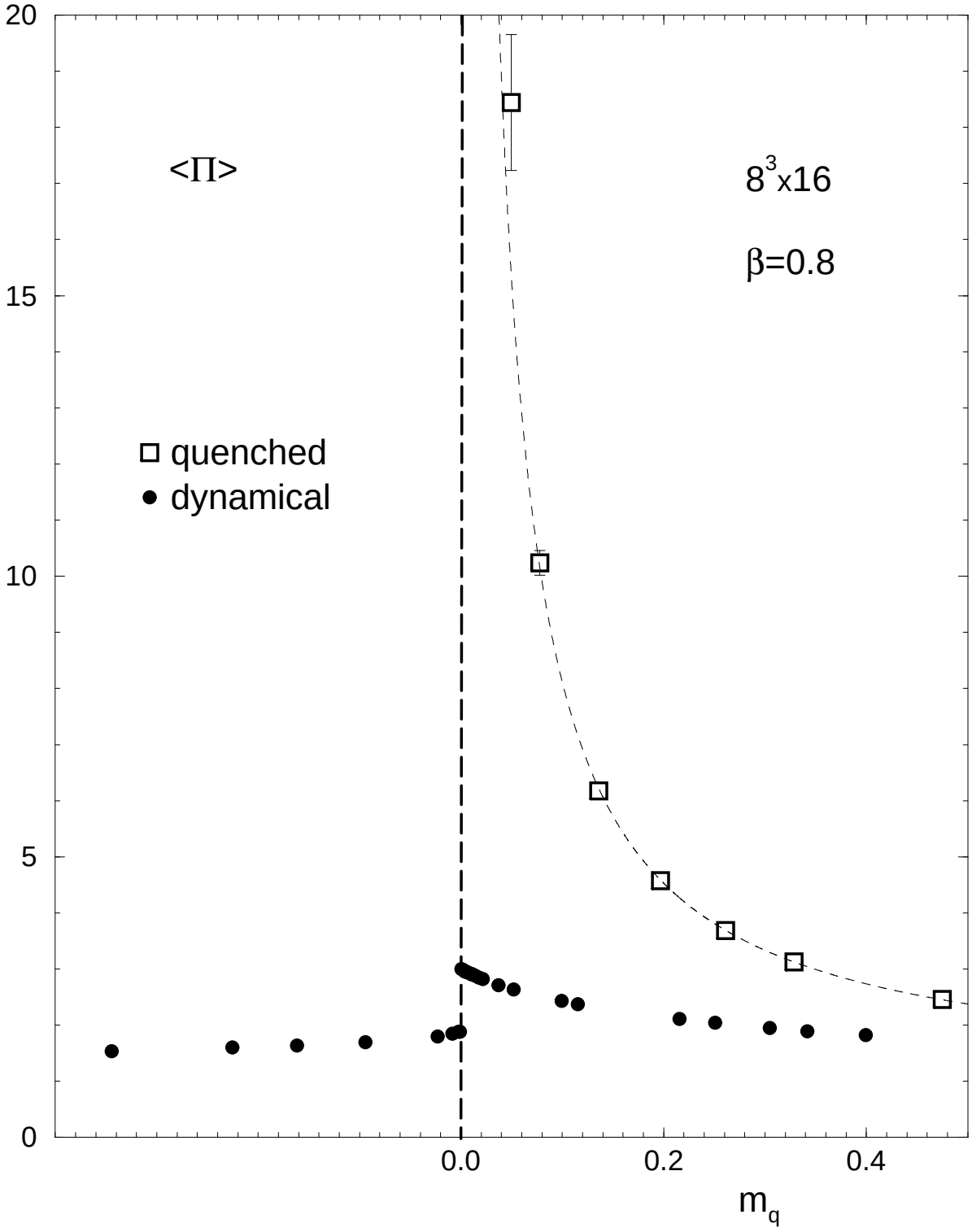

Figure 3: Counterpart to Figure 1 at $\beta = 0.8$.

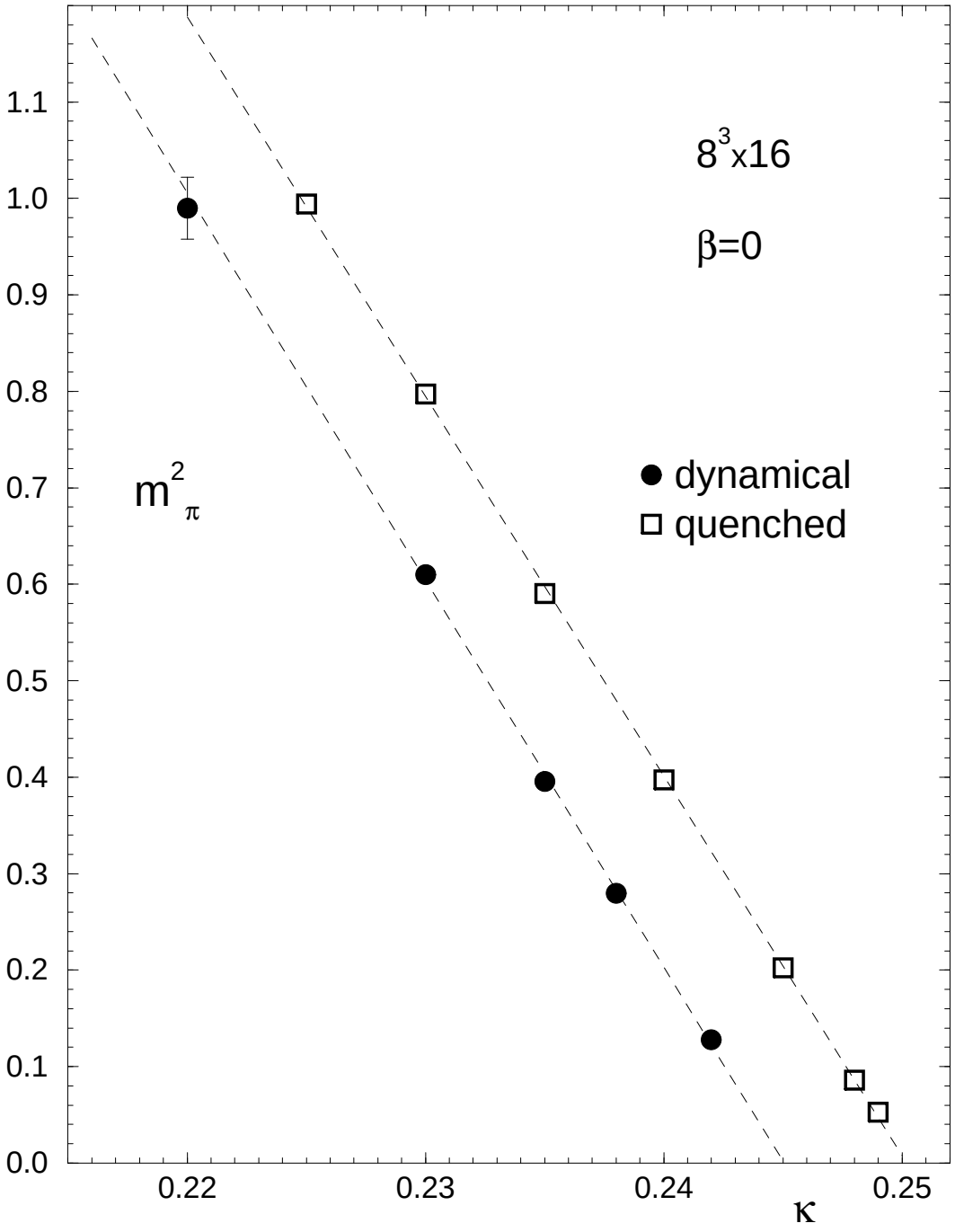

Figure 4: The κ–dependence of m_π^2 for the quenched and dynamical theories at $\beta = 0$ on an $8^3 \times 16$ lattice. The broken lines represent linear fits.

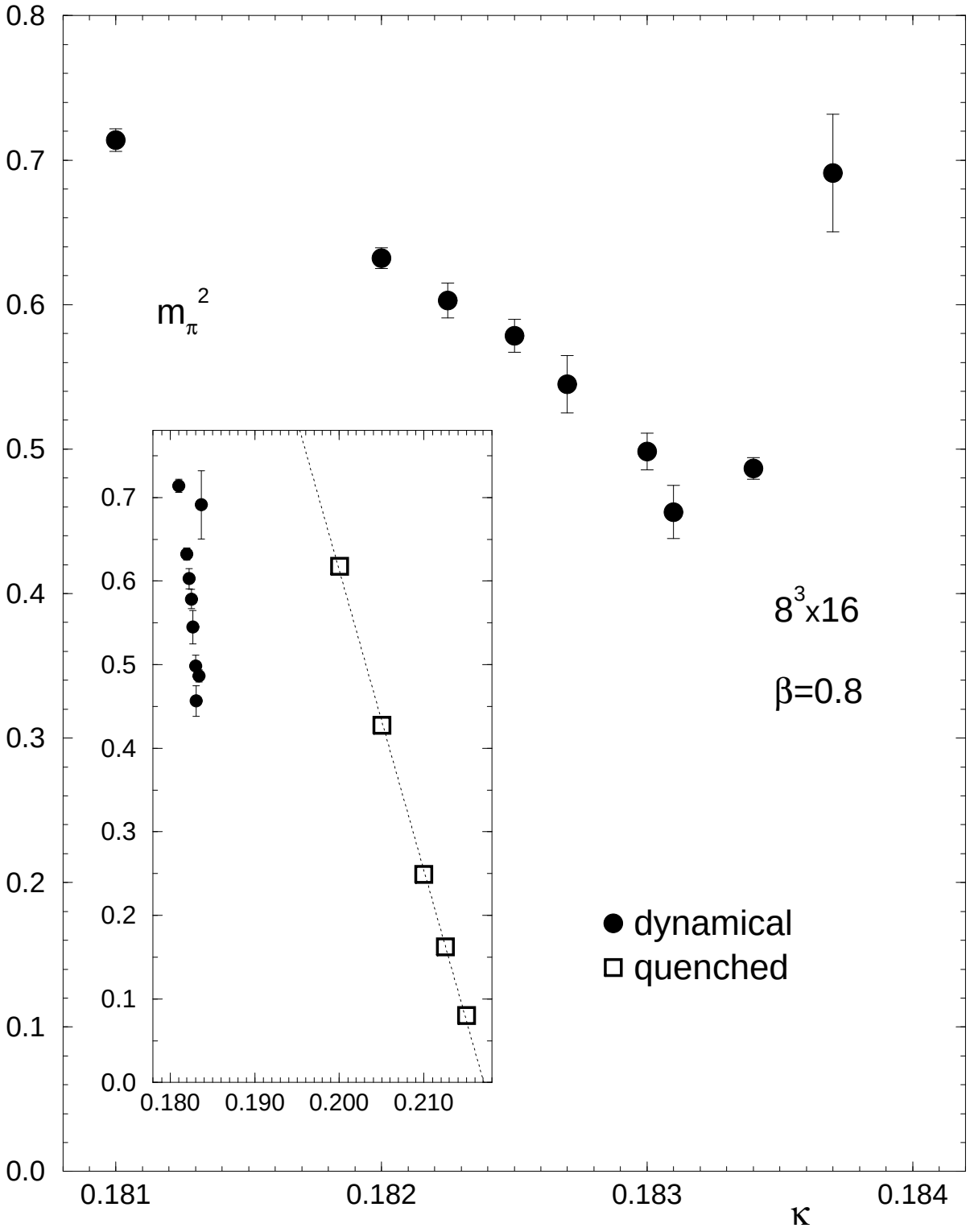

Figure 5: The behavior of m_π^2 around κ_c at $\beta = 0.8$. The κ-scale of the smaller plot is condensed in order to permit a direct comparison between the dynamical and quenched data. The straight line corresponds to a linear fit of the quenched data.